FOCUSED ISSUE FEATURE

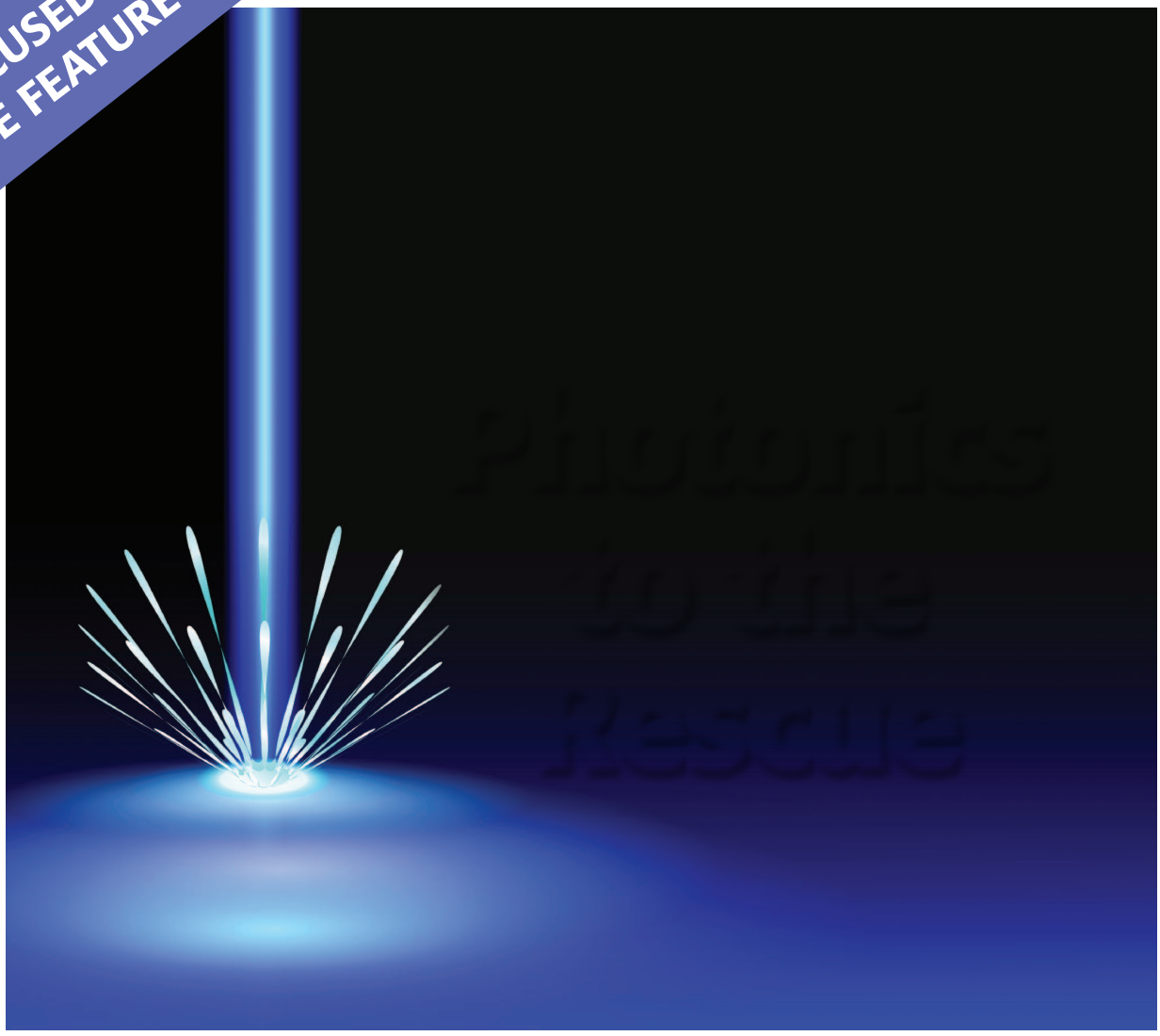

©ISTOCKPHOTO.COM/SCHLEGELFOTOS

A Fresh Look at Microwave Photonic Filters

Jianping Yao

Extensively researched in recent years, microwave photonic filters can be implemented either in an incoherent operational regime or in a coherent operational regime. In the incoherent regime, a delay-line configuration is usually used with a finite-impulse response (FIR) or infinite-impulse response (IIR); to avoid optical interference, an incoherence light source or a laser array is used. Filter tuning and reconfiguration are achieved by changing the time delay and the tap coefficients. In the coherent regime, however, a single wavelength is needed, and the filter's spectral response is translated directly from the spectral response of an optical filter. Thus, a coherent microwave filter requires a well-defined optical filter with a precisely controlled spectral response. This article reviews the techniques for implementing both incoherent and coherent tunable and reconfigurable microwave photonic filters.

Jianping Yao (jpyao@eecs.uottawa.ca) is with the Microwave Photonics Research Laboratory, School of Electrical Engineering and Computer Science, University of Ottawa, Ontario, Canada.

Digital Object Identifier 10.1109/MMM.2015.2441594
Date of publication: 7 August 2015

Incoherent Microwave Photonic Filters

Implementing microwave filters in the optical domain by taking advantage of the low loss and large bandwidth offered by modern photonics has been a topic of interest in recent years, and numerous techniques have been proposed [1]–[6]. An incoherent microwave photonic filter is usually implemented using a delay-line configuration with an FIR or IIR. The multiple taps are realized using either a sliced broadband light source or a laser array, with the time delay between two adjacent taps achieved by passing a microwave-modulated optical signal through optical paths having different physical lengths or traveling in a single fiber or waveguide with linearly chromatic dispersion.

Figure 1 shows a diagram of a delay-line microwave photonic filter with an FIR. It consists of a light source; a modulator, which can be a Mach–Zehnder modulator (MZM) or a phase modulator (PM); a delay-line module; and a photodetector (PD). The key device in a microwave photonic filter is the optical delay-line module, which can be implemented using an array of fiber Bragg gratings (FBGs), an arrayed waveguide, a chirped FBG (CFBG), or a dispersive fiber.

For an N-tap delay-line microwave photonic filter with an FIR, the microwave signal at the output of the PD is given by

$$y(t) = b_0 x(t) + b_1 x(t-T) + b_2 x(t-2T) + \cdots + b_{N-1} x(t-(N-1)T), \quad (1)$$

where $b_0, b_1, b_2, \ldots, b_{N-1}$ are the coefficients of the N taps and T is the time delay between two adjacent taps. By applying a Fourier transform to (1), we have

$$Y(j\omega) = b_0 X(j\omega) + b_1 e^{j\omega T} X(j\omega) + b_2 e^{j\omega 2T} X(j\omega) + \cdots + b_{N-1} e^{j\omega(N-1)T} X(j\omega). \quad (2)$$

The transfer function of the microwave photonic filter is

$$H(j\omega) = \frac{Y(j\omega)}{X(j\omega)} = b_0 + b_1 e^{j\omega T} + b_2 e^{j\omega 2T} + \cdots + b_{N-1} e^{j\omega(N-1)T}. \quad (3)$$

Figure 2(a) shows the spectral response of a four-tap microwave photonic filter with four coefficients of (1, 1, 1, 1). Since all the coefficients are positive, the spectral response has a baseband resonance at zero frequency, and the filter is a low-pass filter. The time delay between two adjacent taps is 125 ps, corresponding to a free spectral range (FSR) of 8 GHz, where FSR $= 1/T$. Figure 2(b) shows the spectral response of a four-tap microwave photonic filter with four coefficients of (1, −1, 1, −1). Since two coefficients are negative, the filter is a bandpass filter with the central frequency of the passband at 4 GHz.

To avoid optical interference, delay-line microwave photonic filters are usually implemented in the incoherent regime. Figure 3 shows two microwave photonic filter configurations operating in the incoherent regime,

To avoid optical interference, delay-line microwave photonic filters are operating in the incoherent regime.

based on a broadband light source and a laser array. In Figure 3(a), a broadband light source is modulated by an RF signal at a modulator and sent to an array of FBGs. The modulated light is then sliced by the FBGs in the

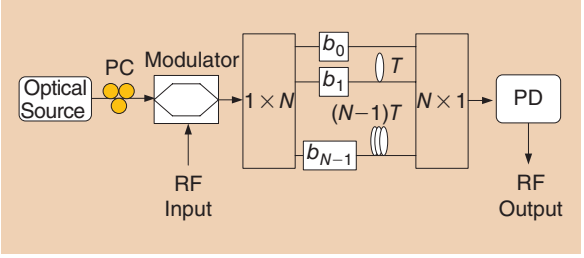

Figure 1. *A delay-line microwave photonic filter with an FIR [4]. PC: polarization controller.*

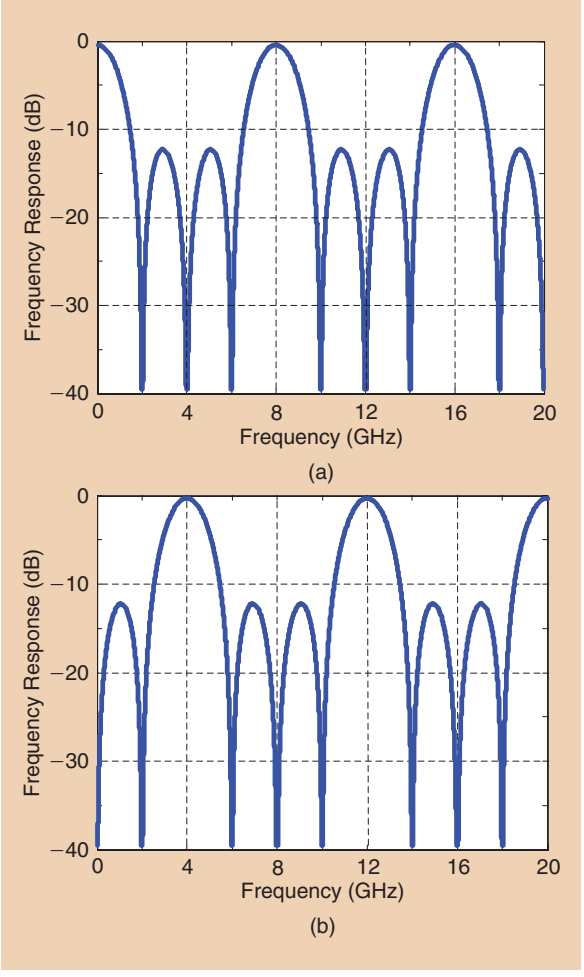

Figure 2. *The spectral response of a four-tap microwave photonic filter with four coefficients of (a) (1, 1, 1, 1) and (b) (1, −1, 1, −1). The time delay between two adjacent taps is 125 ps, corresponding to an FSR of 8 GHz.*

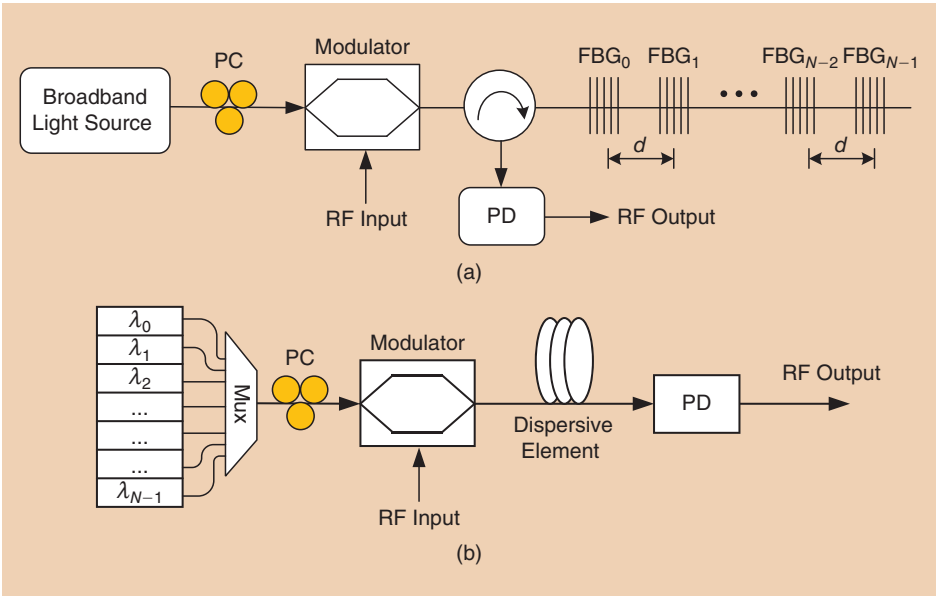

Figure 3. *Two microwave photonic filter configurations operating in the incoherent regime based on (a) a broadband light source and (b) a laser array [4].*

array and reflected via an optical circulator (OC) to a PD. The physical spacing between two adjacent FBGs determines the time delay, and the reflectivities of the FBGs determine the coefficients of the taps.

In Figure 3(b), N wavelengths from a laser array are multiplexed at a wavelength multiplexer and modulated by an RF signal at a modulator, and the modulated-signal is then sent to a dispersive element, which can be a length of dispersive fiber. If the dispersion parameter of the dispersive fiber is D (ps/nm km), the length of the dispersive fiber is L, and the wavelength spacing between two adjacent wavelengths is $\Delta\lambda$, then the time delay between two adjacent taps is $T = \Delta\lambda DL$. For example, for a standard single-mode fiber (SMF), $D = 17$ ps/nm km; if $\Delta\lambda = 0.735$ nm and $L = 10$ km, the time delay is $T = 125$ ps, and the FSR is 8 GHz. To reduce the size of the dispersive element, we may replace the dispersive fiber with a CFBG or with a highly dispersive photonic crystal delay line. Achieving the same time delay of 125 ps requires a CFBG with a length of 125 mm or a photonic crystal delay with an ultrashort length of 2.5 mm [7].

Tuning the filter spectral response is accomplished by tuning the time delay or the wavelength spacing. For the configuration shown in Figure 3(a), the time delay is fixed once the FBG delay line is fabricated, so tuning is rather difficult. For the configuration in Figure 2(b), tuning can be performed by tuning the wavelength spacing. For a wavelength-tunable laser array, the tuning speed can be as high as microseconds. Certain applications, however, require an even faster tuning speed, in the nanosecond range, which can be achieved using a tunable optical comb. A demonstration of an optical comb tunable at a speed of 40 ns was recently reported [8].

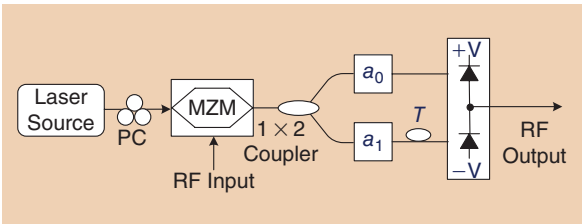

Figure 4. *A delay-line microwave photonic filter with a negative coefficient using differential detection [4].*

It is known that a delay-line microwave photonic filter operating in the incoherent regime would have all-positive tap coefficients [4]–[6]. Based on signal processing theory, an all-positive-coefficient microwave delay-line filter would only operate as a low-pass filter. To overcome this limitation, considerable efforts have been made to design a delay-line microwave photonic filter with negative or complex tap coefficients to achieve arbitrary filtering functionality in the incoherent regime.

Delay-Line Microwave Photonic Filters with Negative Coefficients

A simple approach to producing negative coefficients is to use differential detection [9]. As shown in Figure 4, a light wave from a laser source is modulated by an RF signal at an MZM. The modulated optical signal is time delayed by optical fiber delay lines with a time delay difference between two adjacent taps of T. The time-delayed signals from the fiber delay lines are fed into a differential detection module, which consists of two matched PDs, with the detected microwave signals combined and subtracted electrically, leading to the generation of a positive and a negative coefficient. In this approach, the negative coefficient was not directly generated in the optical domain, and the filter was not all optical, but hybrid. The two-tap photonic microwave delay-line filter shown in Figure 4 can be extended to have multiple taps if the single-wavelength source is replaced by a laser array and the 3-dB coupler is replaced by a wavelength-division multiplexing demultiplexer.

Several techniques have been proposed for implementing delay-line microwave photonic filters with negative coefficients entirely optically. One approach is to use wavelength conversion based on cross-gain modulation

(XGM) in a semiconductor optical amplifier (SOA) [10]. As shown in Figure 5, a tunable laser source (TLS) operating at λ_1 is modulated by an RF signal and then split into two parts. One part goes through an optical fiber to introduce a time delay, and the other part is combined with a continuous-wave (CW) light wave from a laser source operating at a different wavelength λ_2 and then fed into an SOA. Due to the XGM in the SOA, the CW beam λ_2 is also modulated by the input RF signal but with a π phase inversion compared with the RF signal carried by λ_1, which leads to the generation of a negative coefficient. An optical bandpass filter is used to filter out the residual signal at λ_1. Then, the time-delayed microwave signal carried by λ_1 in the upper channel and the π-phase-inverted RF signal carried by λ_2 in the lower channel are combined and detected at a PD. A two-tap microwave photonic bandpass filter with one negative coefficient is thus realized.

Since the two wavelengths are generated by two independent laser sources, the detection at the PD is incoherent. To avoid the beat signal between the two wavelengths falling in the passband of the filter, a large wavelength spacing with a beat frequency that is greater than the bandwidth of the PD should be chosen. For example, if the wavelengths are in the 1,550-nm window and the wavelength spacing is 1 nm, the beat frequency is 125 GHz, which is too high to be detected by the PD.

Negative coefficients can be generated based on two MZMs biased at complementary transmission slopes [11]. The operation of phase inversion is shown in Figure 6. As the figure shows, the two MZMs are biased at the linear regions of the left and the right slopes of the transfer functions. When a microwave signal is applied to the two MZMs, the envelopes of the modulated optical signals are complementary. At the output of a PD, two complementary microwave signals are generated, corresponding to a positive and a negative coefficient. The time delay difference between two adjacent taps is generated due to the chromatic dispersion of a dispersive device.

To implement a delay-line microwave photonic filter with multiple taps, a multiwavelength laser source or a laser array is needed. For those taps with positive and negative coefficients, the corresponding wavelengths must be separately sent to the two MZMs. A similar technique using only a single MZM

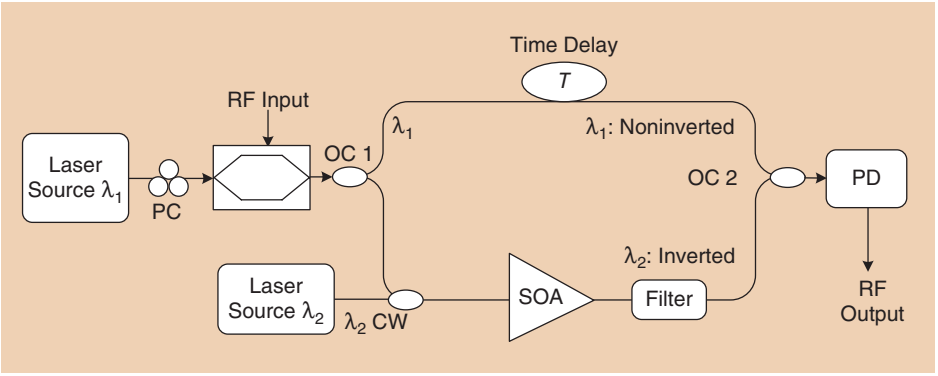

Figure 5. *A delay-line microwave photonic filter with a negative coefficient based on XGM in an SOA [4].*

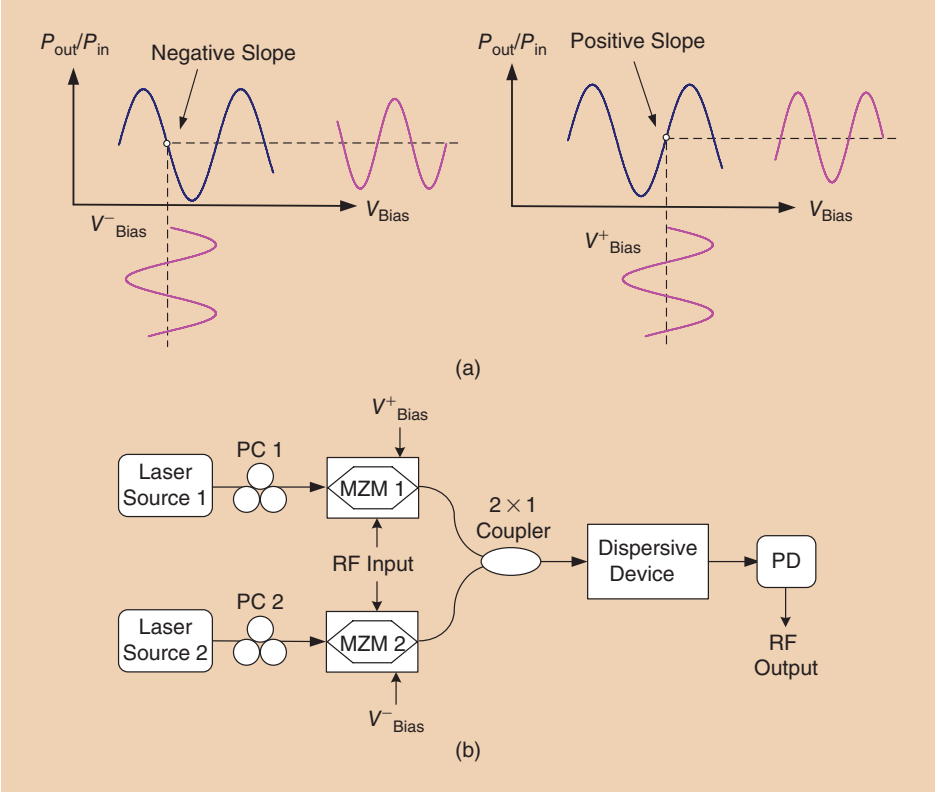

Figure 6. *A delay-line microwave photonic filter with negative coefficients based on phase inversion using complementarily biased MZMs: (a) the phase inversion operation and (b) the filter schematic [4].*

A delay-line microwave photonic filter operating in the incoherent regime would have all-positive tap coefficients.

has been reported [12]. Considering the wavelength dependence of the transfer function of an MZM, a proper dc bias would make the MZM operate at the complementary slopes of the transfer functions when the optical wavelengths are at 1,550- and 1,310-nm windows.

All the filters discussed so far are implemented based on the use of one or multiple MZMs. A delay-line microwave photonic filter with negative coefficients can also be implemented based on a PM [13] [14]. The negative coefficients are generated based on phase modulation to intensity modulation (PM–IM) conversion in dispersive elements with complementary dispersions, such as linearly CFBGs (LCFBGs) with complementary chirps, by reflecting the phase-modulated optical signals from the LCFBGs with positive or negative chirps; microwave signals with or without π phase inversion are generated at the PD. An added advantage of using an optical PM is that no dc bias is needed, which eliminates the bias drifting problem that exists in an MZM.

This operation is shown in Figure 7(a). An RF signal is applied to a PM via the RF port to phase-modulate the multiple wavelengths applied to the PM via the optical port. Since a PD functions as an envelope detector, if a phase-modulated signal is directly applied to a PD, no modulating signal will be recovered except a dc. This conclusion can also be explained based on the spectrum of a phase-modulated signal.

As shown in Figure 7(a), a phase-modulated signal under small-signal modulation conditions has two sidebands (+1 and −1 order) and an optical carrier with the +1 and −1 order sidebands out of phase. The beating between the optical carrier and the +1 order sideband will exactly cancel the beating between the optical carrier and the −1 order sideband. However, if the phase-modulated optical signal passes through a dispersive element, the phase relationship between the two sidebands and the optical carrier will be changed, leading to the conversion from PM to IM. In addition, depending on the sign of the chromatic dispersion (positive or negative), a recovered RF signal with or without a π phase inversion would be generated, which would lead to the generation of negative coefficients. The system configuration of the filter is shown in Figure 7(b).

Negative coefficients can also be generated using a polarization modulator (PolM) [15], [16]. A PolM is a special PM that supports both transverse electric and transverse magnetic modes, but with opposite phase modulation indices. Figure 8(a) shows the operation in principle. A light wave from a laser source is sent to a PolM via a polarization controller (PC) with its polarization direction aligned to have a 45° angle with respect to one principal axis of the PolM, which is modulated by an input RF signal. Thanks to the polarization modulation at the PolM, two out-of-phase RF signals carried by two optical carriers with identical wavelengths but orthogonal polarizations are achieved at the output of the PolM. The optical microwave signals are fed into a section or two sections of polarization-maintaining fiber (PMF) to produce a delay line with two or four time delays. A microwave photonic bandpass filter of two or four taps with one

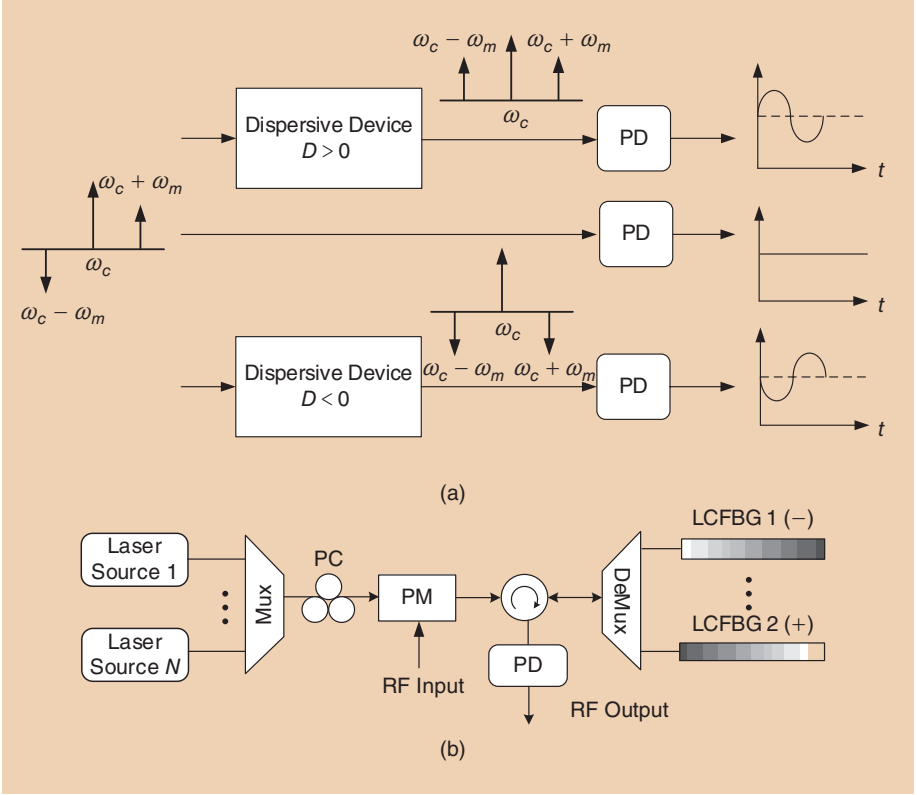

Figure 7. *(a) RF phase inversion based on PM–IM conversion through opposite dispersions. (b) A delay-line microwave photonic filter with a negative coefficient based on PM–IM conversion in two LCFBGs with opposite dispersions [4].*

or two negative coefficients has been demonstrated [15].

For implementations of a delay-line microwave photonic filter with an arbitrary number of taps and arbitrary tap coefficients, a modified structure based on a PolM is shown in Figure 8(b) [16]. Instead of using a single-wavelength light source, an array of N wavelengths is employed. An optical polarizer is connected at the output of the PolM with its transmission axis aligned at an angle of 45° to one principal axis of the PolM. By adjusting the polarization directions of the input light waves to be 45° or 135° to one principal axis of the PolM, an in-phase or out-of-phase intensity-modulated optical microwave signal is obtained at the output of the optical polarizer, which leads to the generation of a negative or positive coefficient. The time-delay difference between adjacent taps is generated by using a dispersive delay line, such as a dispersive fiber or a CFBG.

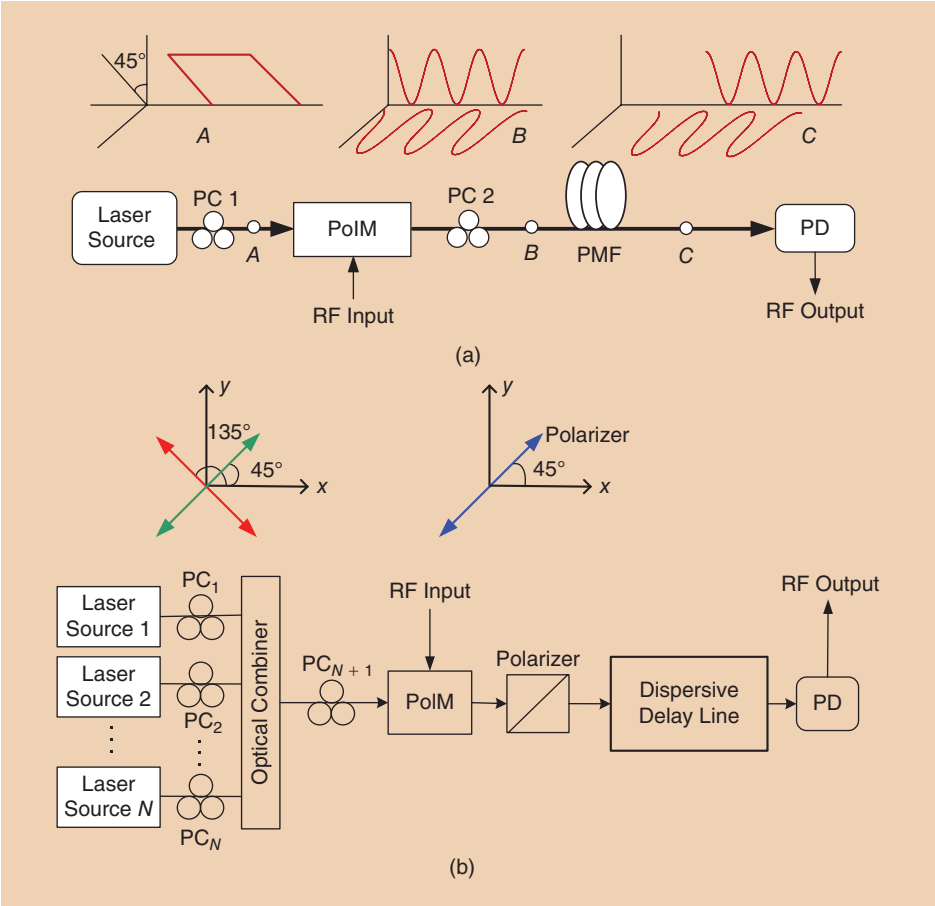

Figure 8. *A delay-line microwave photonic filter with negative coefficients based on a PolM: (a) a delay-line microwave photonic filter based on a PolM using a single wavelength with time delays generated by a section or two sections of PMF and (b) a delay-line microwave photonic filter based on a PolM using N wavelengths with an arbitrary number of taps and arbitrary tap coefficients [4].*

Delay-Line Microwave Photonic Filters with Complex Coefficients

Frequency tuning of a delay-line microwave photonic filter is achieved by tuning the time-delay difference. However, the change of the time-delay difference leads to the change of the FSR, which would result in the 3-dB bandwidth being changed as well as a change in the entire shape of the frequency response. For many applications, however, it is expected that only the center frequency of the passband or stopband is changed, while the spectral shape remains unchanged. A solution to this problem is to implement a delay-line microwave photonic filter with complex coefficients.

An N-tap microwave delay-line filter with complex coefficients should have a transfer function given by

$$H(\omega) = a_0 + a_1 e^{-j\theta} \cdot e^{-j\omega T} + \cdots + a_{N-1} e^{-j(N-1)\theta} \cdot e^{-j\omega(N-1)T} = \sum_{n=0}^{N-1} a_n e^{-jn\theta} \cdot e^{-j\omega nT}, \quad (4)$$

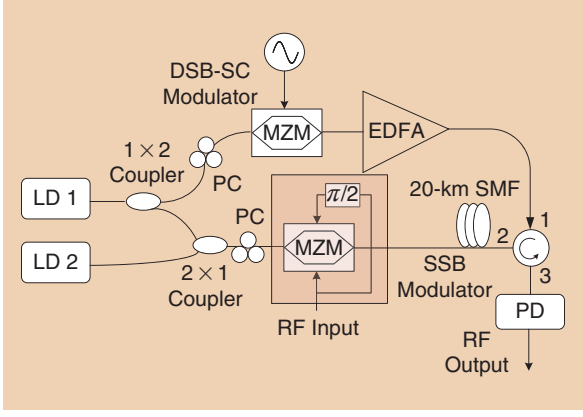

Figure 9. *A two-tap delay-line microwave photonic filter with a complex coefficient based on SSB modulation and SBS [4]. LD: laser diode.*

where T is the time delay difference between two adjacent taps. To tune the filter while maintaining the shape of the frequency response, the phase shifts of all the taps should maintain a fixed relationship, as can be observed from (4). Therefore, the phase shift of each tap should be tuned independently.

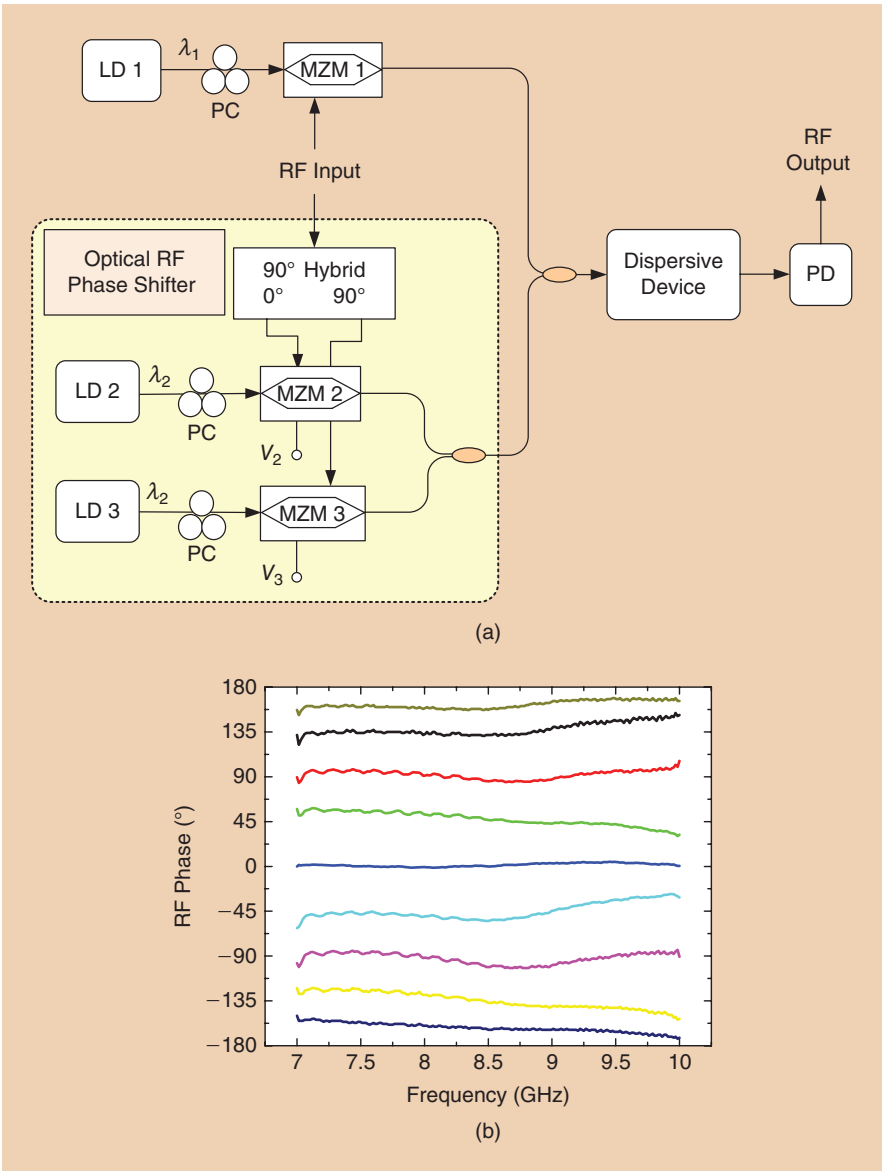

Figure 10. *A delay-line microwave photonic filter with a complex coefficient generated based on an optical RF phase shifter: (a) the system architecture and (b) the measured phase shifts for different bias voltages over a large microwave frequency band. The phase shifts are independent of the microwave frequency [4].*

In [17], a tunable delay-line microwave photonic filter with a complex coefficient was reported, in which a complex coefficient was generated by changing the phase of the RF signal; this was realized based on a combined use of optical single-sideband (SSB) modulation and stimulated Brillouin scattering (SBS). The system setup is shown in Figure 9. It was demonstrated that the phase of a microwave signal carried by an optical carrier will experience a phase shift if the spectrum of the optical carrier falls in the SBS gain spectrum when passing through an optical fiber in which an SBS effect results [18].

In [17], since the generation of a complex coefficient involves the use of a high-power erbium-doped fiber amplifier (EDFA) to trigger the SBS as well as an additional MZM and a long fiber, the system is extremely complicated, consuming considerable power at a high cost. A simplified configuration reported in [19] generates a complex coefficient using a wideband-tunable optical RF phase shifter that consists of two MZMs, as shown in Figure 10(a). The phase of the RF signal is shifted by simply adjusting the bias voltages applied to the two MZMs, and the phase shift remains constant over the entire microwave spectrum of interest. Figure 10(b) shows the measured phase shifts for different bias voltages over a large microwave frequency band. As can be observed, the phase shifts are independent of the microwave frequency.

Nonuniformly Spaced Delay-Line Microwave Photonic Filters

The microwave photonic filters in [17] and [19] are very complicated, especially with a large number of taps. For a simpler structure, a new concept was proposed that generates complex coefficients based on nonuniformly spaced taps. It was demonstrated that the complex coefficients can be equivalently generated by introducing additional time delays to the taps [20].

A uniformly spaced microwave delay-line filter has an impulse response $h_R(t)$ given by

$$h_R(t) = \sum_{k=0}^{N-1} \alpha_k \delta(t - kT), \tag{5}$$

where N is the number of taps, a_k is the filter coefficient of the kth tap, $T = 2\pi/\Omega$ is the time delay difference between two adjacent taps, and Ω is the FSR of the filter. By applying the Fourier transform to (5), we have the frequency response of the filter given by

$$H_R(\omega) = \sum_{k=0}^{N-1} \alpha_k \ \exp\left(-jk\frac{2\pi}{\Omega}\omega\right). \tag{6}$$

It is known that $H_R(\omega)$has a multichannel frequency response with adjacent channels separated by an FSR, and with the mth channel located at $\omega = m\Omega$. Note that

except for the different central frequencies, the frequency responses for all the channels are exactly identical.

In a delay-line microwave photonic filter based on incoherent detection, the coefficients are usually all positive; otherwise, special designs have to be incorporated to generate negative or complex coefficients. However, a phase term can be introduced into a specific coefficient by adding an additional time delay at a specific tap, and we call this a time-delay-based phase shift [20]. For example, at $\omega = m\Omega$, a time delay shift of $\Delta\tau$ will generate a phase shift given by $\Delta\varphi = -\Delta\tau \times m\Omega$. Note that such a phase shift is frequency dependent, which is accurate only for the frequency at $m\Omega$ but approximately accurate for a narrow frequency band at around $m\Omega$.

For most applications, the filter is designed to have a very narrow frequency band. Therefore, for the frequency band of interest, the phase shift can be considered constant over the entire bandwidth. As a result, if the mth bandpass response, where $m \neq 0$, is considered, one can then achieve the desired phase shift at the kth tap by adjusting the time delay shift by $\Delta\tau_k$. Considering the time delay shift of $\Delta\tau_k$, one can get the frequency response of the nonuniformly spaced delay-line filter at around $\omega = m\Omega$:

$$\begin{aligned} H_N(\omega) &= \sum_{k=0}^{N-1} \alpha_k \exp\left[-j\left(k\frac{2\pi}{\Omega} + \Delta\tau_k\right)\omega\right] \\ &= \sum_{k=0}^{N-1} \alpha_k \exp(-j\omega\Delta\tau_k) \times \exp\left(-jk\frac{2\pi}{\Omega}\omega\right) \\ &\approx \sum_{k=0}^{N-1} [\alpha_k \exp(-jm\Omega\Delta\tau_k)] \times \exp\left(-jk\frac{2\pi}{\Omega}\omega\right). \quad (7) \end{aligned}$$

As can be observed from (7), it is possible to get an equivalent phase shift (EPS) for each tap coefficient. Specifically, if the desired phase shift for the kth tap is φ_k, the total time delay τ_k for the kth tap is $\tau_k = kT - \varphi_k/m\Omega$. As a result, if the time delay of each tap is adjusted, the filter coefficients will have the required phase shifts to generate the required passband with the desired bandpass characteristics.

In [20], a seven-tap delay-line microwave photonic filter with nonuniformly spaced taps to produce a flat-top bandpass frequency response was demonstrated. The experimental setup is shown in Figure 11(a). Assuming that the passband of interest is at $m = 1$ and the frequency response of the bandpass has the shape of a rectangle, then the corresponding impulse response should be a sinc function, which has both positive and negative values extending to infinity along the horizontal axis. For practical implementation, the calculated impulse response should be cut off to enable a physically realizable filter. If a regular delay-line microwave photonic filter is employed to produce the frequency response, the filter coefficients can be selected to be [−0.12, 0, 0.64, 1, 0.64, 0, −0.12]. The frequency response is shown as the dotted line in Figure 11(b), where $T = 82.6$ ps, which corresponds to an FSR of 12.1 GHz. The 3-dB bandwidth of the filter is 5.0 GHz with a central frequency of 12.1 GHz.

The key device in a microwave photonic filter is the optical delay-line module.

The same bandpass characteristics at $m = 1$ can be generated by using nonuniform spacing with all-positive coefficients of [0.12, 0, 0.64, 1, 0.64, 0, 0.12]. The time delays for the seven taps are then $[-2.5T, -2T, -T, 0, T, 2T, 2.5T]$. As the figure shows, the taps are nonuniformly spaced. Since at $m = 0$ there are no phase shifts introduced into the taps, there is always a baseband resonance that was eliminated by using an optical PM to produce a notch at the baseband [21], [22]. The frequency response of the PM–IM conversion is designed so that its first peak is located at $f = 12.1$ GHz, which is shown as the dashed-dotted line in Figure 11(b). The overall frequency response of the nonuniformly spaced filter is calculated and shown as the solid line in Figure 11(b). A flat-top frequency response is achieved in a delay-line microwave photonic filter with all-positive

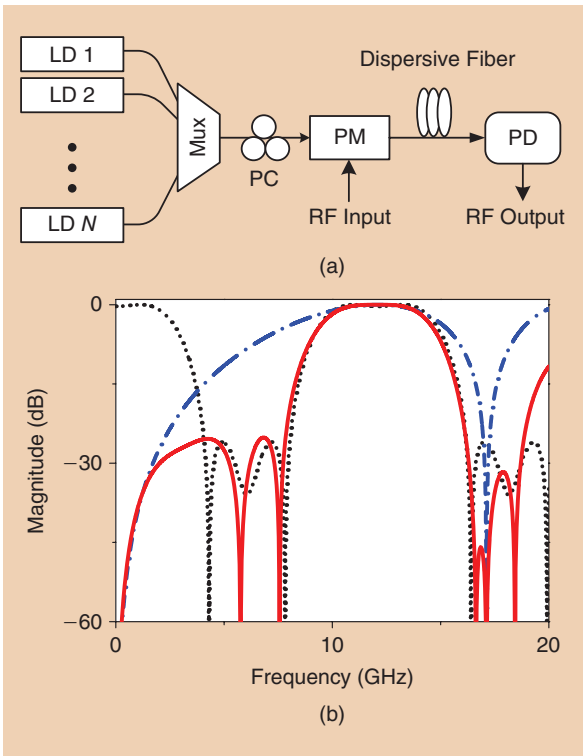

Figure 11. *(a) A nonuniformly spaced delay-line microwave photonic filter. (b) Frequency versus magnitude. Dotted line: the frequency response of a regular delay-line microwave photonic filter with true positive and negative coefficients. Dashed-dotted line: the frequency response of the PM-IM conversion. Solid line: the frequency response of the nonuniformly spaced delay-line microwave photonic filter [4].*

A microwave photonic filter can also be implemented in the coherent regime using a single-wavelength light source.

coefficients. The 3-dB bandwidth was 4.9 GHz, and the central frequency was 12.1 GHz.

A comprehensive study of the design of a nonuniformly spaced microwave delay-line filter was reported in [23]. This technique is particularly useful for applications such as arbitrary microwave waveform generation and microwave pulse compression. The concept has been employed to implement RF pulse phase encoding [24]. The concept has also been employed to implement a delay-line microwave photonic filter with a quadratic phase response for chirped microwave pulse generation [25] and pulse compression [26].

Coherent Microwave Photonic Filters

The delay-line microwave photonic filters discussed so far belong to a incoherent microwave photonic filters, where optical interference is eliminated by using either a broadband incoherent light source or a laser array. In fact, a microwave photonic filter can also be implemented in the coherent regime using a single-wavelength light source. Since a coherent microwave photonic filter does not have a delay-line configuration, optical interference is not an issue that would affect the stable operation of the filter.

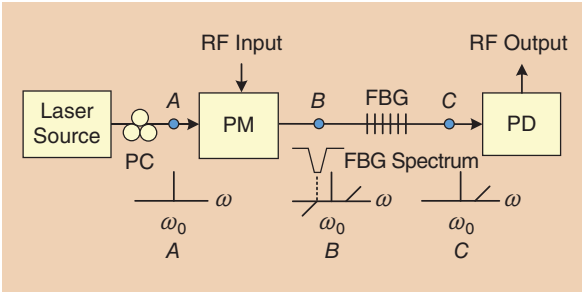

Figure 12. *A coherent microwave photonic filter, in which an optical notch filter is used to filter out one sideband of a phase-modulated signal, thus achieving PM–IM conversion.*

A general structure of a coherent microwave photonic filter is shown in Figure 12. A narrow-linewidth light wave from a laser source is sent to a PM. Assuming small-signal modulation, at the output of the PM, an optical carrier and two sidebands are generated. Note that for phase modulation, the two sidebands are out of phase. Thus, detecting a phase-modulated signal directly at a PD will not generate an RF signal except a dc since the beating between the optical carrier and the lower sideband will completely cancel the beating between the optical carrier and the upper sideband. However, if one of the sidebands is removed by an optical notch filter in transmission or by using a dual-passband filter in reflection [27], such as an FBG or two cascaded FBGs, then the phase-modulated signal is converted into an SSB intensity-modulated signal, and the detection of the SSB intensity-modulated signal at a PD will generate an RF signal.

Figure 12 shows a coherent microwave photonic filter, in which an optical notch filter is used to filter out one sideband of a phase-modulated signal, thus achieving PM–IM conversion. As can be observed, the entire operation is equivalent to a microwave filter, with the bandwidth determined by the bandwidth of the notch of the optical notch filter (an FBG). The center frequency is determined by the wavelength spacing between the optical carrier and the center wavelength of the notch. Thus, by simply tuning the center frequency of the notch filter or the wavelength of the laser source, the center frequency of the microwave bandpass filter can be tuned. During tuning, the spectral shape is kept unchanged. This offers a distinct advantage compared with an incoherent microwave photonic filter, where the spectral shape changes when the filter is tuned unless complex coefficients are used to avoid such a spectral shape change, as previously discussed.

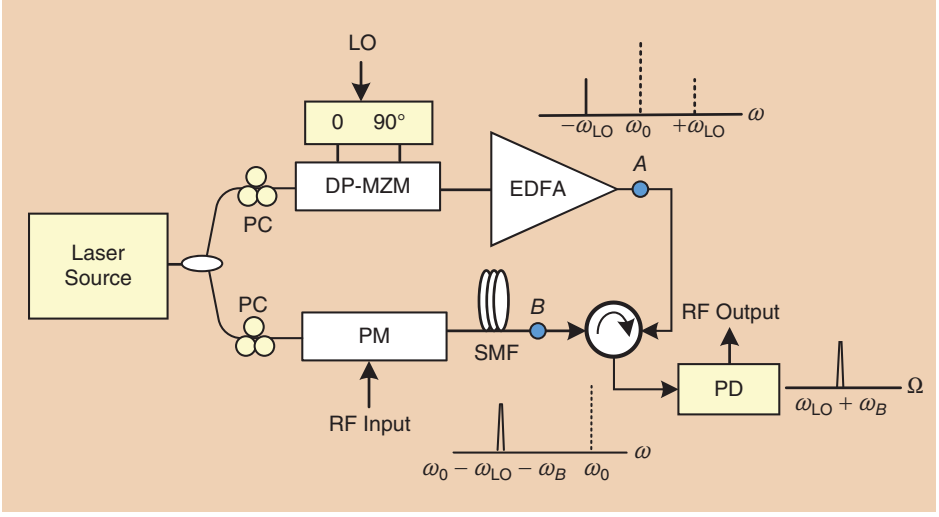

Figure 13. *A coherent microwave photonic filter implemented based on phase modulation and PM–IM using SBS gain.*

In [27], instead of using a single FBG in transmission, two cascaded FBGs are used in reflection with one FBG to select the optical carrier and the other FBG

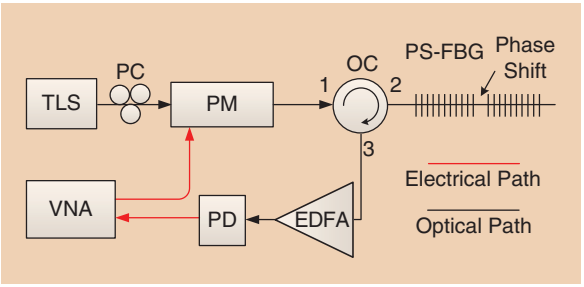

Figure 14. *A coherent microwave photonic filter implemented based on phase modulation and PM–IM conversion using a PS-FBG [31].*

to select one sideband; a phase-modulated signal is converted into an SSB intensity-modulated signal. A microwave photonic filter with a spectral shape identical to the notch of the second FBG is generated. The major limitation of the technique in [27] is the large passband since a uniform FBG was employed. The passband of the microwave photonic filter is determined by the bandwidth of the FBG to select the sideband. Using a ring resonator [28], the passband can be smaller, but it is still too large for most applications.

Due to the ultranarrow bandwidth of an SBS gain or loss spectrum, a microwave photonic filter with narrow passband can be implemented based on phase modulation and PM–IM conversion using this spectrum. Figure 13 shows a configuration to implement a narrowband microwave filter based on SBS. A light wave from a laser source at ω_0 is split into two paths. At the upper path, the light is modulated by a local oscillator (LO) signal at a dual-parallel MZM (DP-MZM) to generate an SSB with suppressed carrier (SSB-SC) signal. Assuming that the frequency of the LO signal is ω_{LO}, the generated lower sideband is at $\omega_0 - \omega_{LO}$. The SSB-SC signal is sent to an EDFA to increase its power and then launched into an SMF to stimulate the SBS effect.

The SBS gain and loss are located at $\omega_O - \omega_{LO} - \omega_B$ and $\omega_O - \omega_{LO} + \omega_B$. If one sideband of a phase-modulated signal is amplified by the SBS gain, then the phase-modulated signal is converted into an intensity-modulated signal, and the detection of the intensity-modulated signal at a PD will generate a microwave signal at $\omega_{LO} - \omega_B$, as shown in Figure 13. The entire operation of the system is equivalent to a microwave bandpass filter, with the passband determined by the SBS gain spectrum.

The advantage of this approach is that the filter can be tunable by tuning the LO frequency, and the passband is very narrow. However, the system is quite complicated, especially because a high-power EDFA and a long SMF are needed. A similar configuration can be used to produce a microwave photonic notch filter if the PM is replaced by another DP-MZM to generate unbalanced double-sideband modulation. By removing part of the spectrum from one sideband using the SSB loss to make the amplitude of the sideband at that spectrum identical to that of the other sideband, a notch with an ideally infinite notch depth is

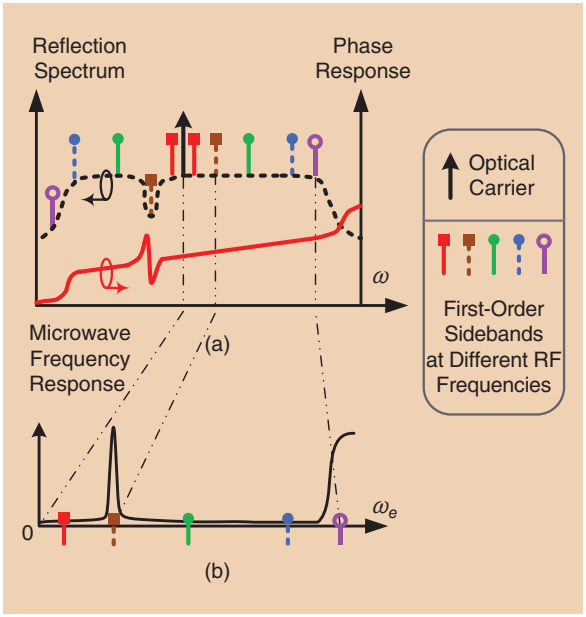

Figure 15. *The operation of a coherent microwave photonic filter. (a) The reflection spectrum (dashed line) and phase response (solid line) of the PS-FBG. (b) The frequency response of the coherent microwave photonic filter [31].*

produced [29]. If the power ratio between the two sidebands of the unbalanced double-sideband modulated signal is continuously controlled, then the microwave notch filter can be tuned with a tunable notch depth, or the notch filter can be controlled to become a bandpass filter with a tunable passband gain [30].

To avoid using SSB that requires a high-power EDFA and a long SMF, one may use an optical filter with an ultranarrow passband. Figure 14 shows the implementation of a coherent microwave photonic filter using a phase-shifted FBG (PS-FBG) to perform PM–IM conversion [31]. A PS-FBG is a special FBG with a phase shift introduced to the FBG during the inscription [31]. For a uniform FBG, if a π phase shift is introduced, an ultranarrow notch with a phase jump in the notch would be generated in the reflection band [32]. If a phase-modulated optical signal injected into the PS-FBG is employed to modify the magnitude and the phase of one sideband, PM–IM conversion would be achieved, which would lead to the implementation of an ultranarrow passband, as shown in Figure 15.

Figure 16 shows the frequency response of a coherent microwave photonic filter using a PS-FBG. The wavelength of the optical carrier is tuned such that the lower sideband falls in the notch of the PS-FBG when the microwave frequency is equal to the difference between the frequency of the optical carrier and the center frequency of the notch. By increasing the wavelength of the optical carrier, the center frequency of the microwave photonic filter is accordingly increased. Figure 16(a) shows the superimposed frequency responses of the microwave photonic filter with a tunable central frequency covering a frequency range of about 15 GHz

The implementation of microwave photonic filters in the coherent regime can have a much simpler configuration.

with a tuning step of 1.45 GHz. As Figure 16(a) shows, the ratio of the transmission peak to the sidelobe can be as large as 40 dB. Figure 16(b) shows a close-up view of the measured frequency response at about 6.9 GHz. The 3-dB bandwidth is about 60 MHz. The bandwidth can be further decreased by using a PS-FBG with a narrower notch.

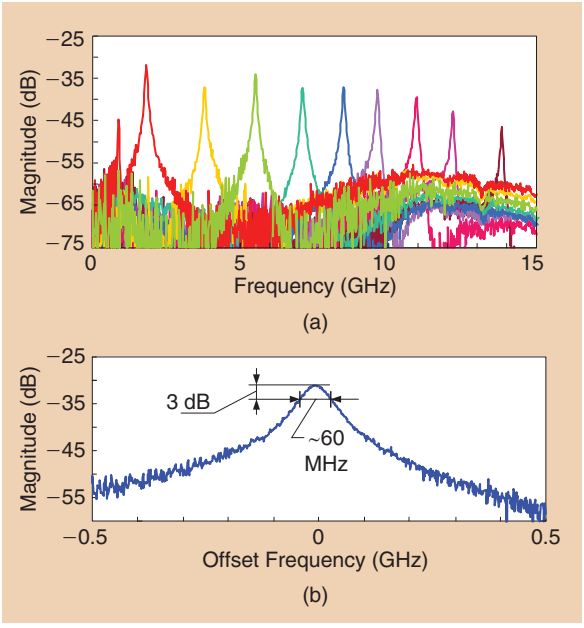

Figure 16. *(a) The measured frequency responses of a coherent microwave photonic filter when the second PS-FBG is employed. (b) A close-up view of the frequency response when the center frequency is tuned at 6.9 GHz [31].*

Coherent Microwave Photonic Filters with a Flat Top

The same basic concept for implementing a coherent microwave photonic filter based on PM–IM conversion to translate the spectral response of an optical filter to that of a microwave photonic filter can be used to implement a microwave photonic filter with a flat top [33]. Instead of using SBS or a PS-FBG, a specially designed superstructured FBG (SFBG) is used. An SFBG is an FBG that is spatially modulated by a periodic sampling function. Due to the spatial sampling, the spectral response has multiple channels. If one period of the sampling function is intentionally increased by a half period, a π phase shift is introduced equivalently to the grating, leading to a narrow notch. The technique is called the EPS technique [34].

To have a flat bottom in the notch, the SFBG is designed with two closely spaced notches; these are achieved by introducing two EPSs into the structure. Each phase shift produces a Lorentz-shaped notch, and the combination of the two closely spaced Lorentz-shaped notches results in a notch with a flat bottom. When the SFBG with a flat-bottom notch is incorporated to perform PM–IM conversion, a passband with a flat top is achieved.

The reflection bandwidth and notch width of the SFBG, which determine the frequency tunable range and bandwidth of the passband, can be controlled by regulating the length and maximum index modulation of the SFBG. Figure 17(a) shows a simulated reflection spectrum of a PS-FBG with a single phase shift, and Figure 17(b) shows a simulated reflection spectrum of an SFBG with two phase shifts. Figure 17(c) shows the structure of an SFBG in which two EPSs are incorporated.

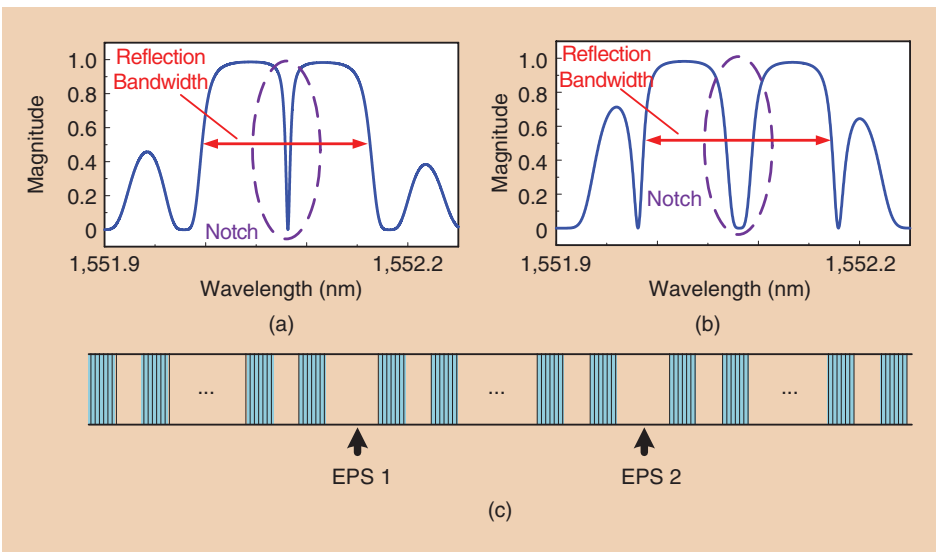

Figure 17. *(a) Simulated reflection spectrum of a PS-FBG with a single phase shift. (b) Simulated reflection spectrum of an SFBG with two phase shifts. (c) The SFBG structure [33].*

Figure 18(a) shows the magnitude and phase response in reflection of an SFBG with a length of 32.4 mm. Due to the limited resolution of the optical vector analyzer, the notch depth and shape cannot be precisely shown. Figure 18(b) shows the frequency response of the microwave photonic filter, which has a narrow passband with a flat top. The flatness of the passband is within ±0.25 dB. The phase response of the microwave photonic

filter is also measured and is shown in Figure 18(b). Here, the phase response is linear in the passband. The 3-dB bandwidth is 143 MHz, the 20-dB bandwidth is 370 MHz, and the shape factor (defined as the ratio between the 20- and 3-dB bandwidths) is calculated to be 2.6, which is much smaller than those reported in [32]. A smaller shape factor represents a better selectivity.

By tuning the wavelength of the optical carrier, the central frequency of the passband is tuned from 0.4 to 6.4 GHz, as shown in Figure 19. The magnitude and bandwidth of the passband remain almost unchanged during tuning, a feature that is important for applications where the loss and bandwidth are required to be constant. The insertion loss is measured to be about 28 dB. The use of a high-power-handling PD may reduce the loss [31]. The spurious free dynamic range (SFDR) of the microwave photonic filter is also measured and is about 83 dB·Hz$^{2/3}$.

Coherent Microwave Photonic Filters with Dual Passbands

For certain applications, microwave filters with dual passbands are needed due to the increasing demand for multiband/multifunctional microwave systems that support various modern services. Such systems require

For certain applications, microwave filters with dual passbands are needed.

microwave circuits and components that can handle several different frequency bands. The same concept already discussed can also be used to implement a microwave photonic filter with two passbands [35].

The key component in a dual-band microwave photonic filter is an equivalent PS-FBG (EPS-FBG), which is designed and fabricated using the EPS technique [34]. The EPS-FBG has multiple channels due to the spatial sampling of the grating structure. EPSs introduced to the ± 1 channels are realized through changing the sampling function. Therefore, the fabrication of an EPS-FBG is significantly simplified, since control of the spatial sampling is in a micrometer scale, while control of the phase shift in the fabrication of a true PS-FBG is in a nanometer scale.

In the design, two π phase shifts are introduced to both of the ± 1 channels to produce an ultranarrow and flat-bottom notch in each channel. Figure 20 shows a simulated reflection spectrum of an EPS-FBG with two π phase shifts. As can be observed, the notches are flat

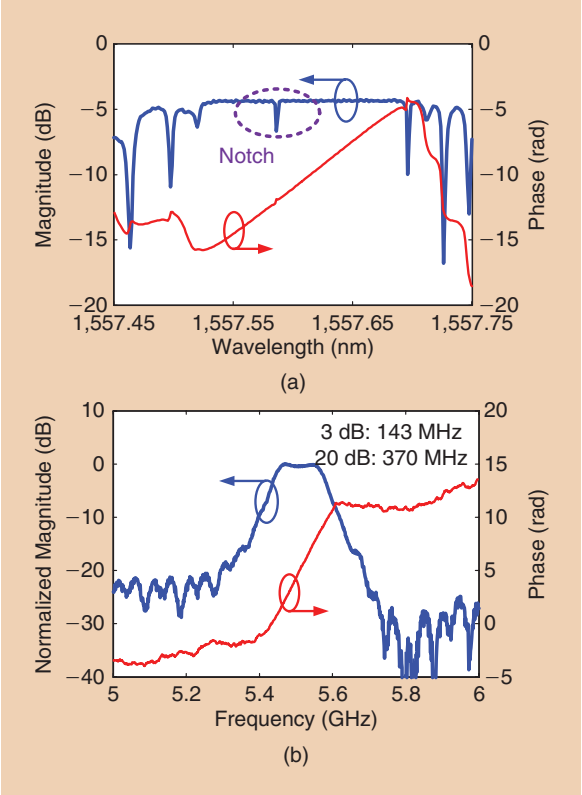

Figure 18. *(a) The measured reflection spectrum and phase response of the SFBG. (b) The frequency response and phase response of the microwave photonic filter using the SFBG [33].*

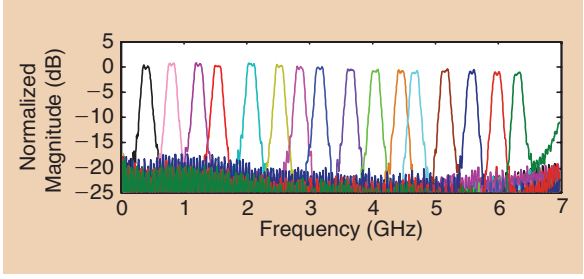

Figure 19. *The measured frequency response of the narrow and flat-top microwave photonic filter with a tunable passband from 0.4 to 6.4 GHz. [33].*

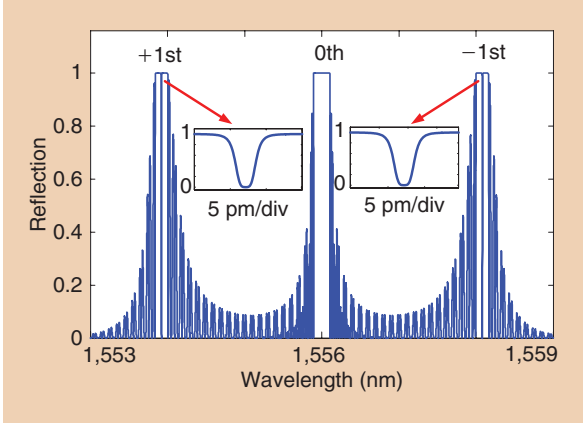

Figure 20. *Simulated reflection spectrum of an EPS-FBG with two phase shifts [35].*

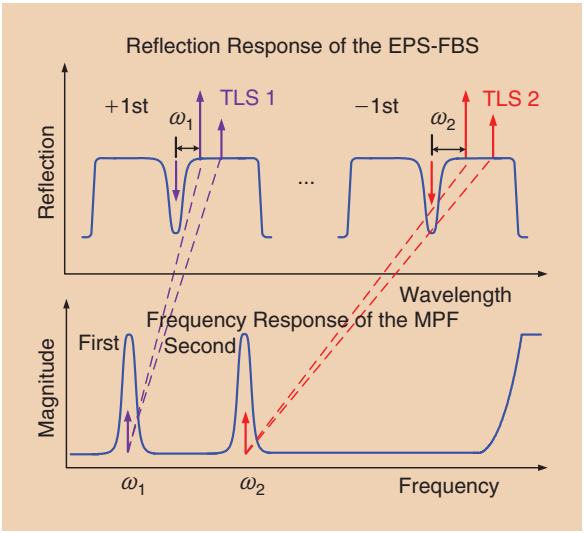

Figure 21. *An illustration of the generation of the two passbands [35].*

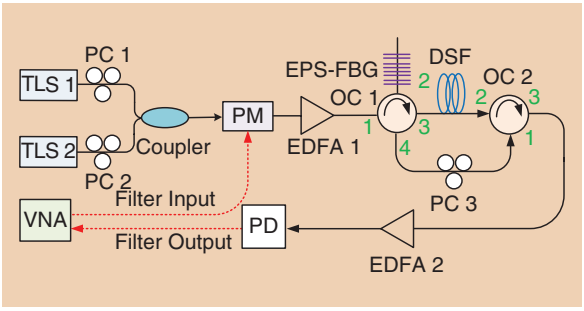

Figure 22. *A schematic of a dual-passband microwave photonic filter [35]. VNA: vector network analyzer.*

due to the use of the two phase shifts. A bandpass filter is achieved due to the PM–IM conversion by filtering out one sideband of a phase-modulated signal. In a dual-band microwave photonic filter, the PM–IM conversion is performed at both the ±1 channels, and thus two independently tunable passbands are generated, as shown in Figure 21. Because two π phase shifts are introduced to achieve flat-bottom notches, the passbands have small shape factors. Here, the shape factor is again defined as the ratio between the 20- and 3-dB bandwidths.

To produce two independent passbands, two optical carriers from two TLSs (TLS 1 and TLS 2) are tuned to locate at the ±1 channels of the EPS-FBG, as shown in Figure 22. When one sideband of a phase-modulated signal is suppressed by the notch in the +1 channel, a passband with a central frequency of ω_1 (the frequency difference between the optical carrier and the notch in the +1 channel) will be produced due to the PM–IM conversion. Similarly, when one sideband of a phase-modulated signal is suppressed by the notch in the −1 channel, a passband with a central frequency of ω_2 (the frequency difference between the optical carrier and the notch in the −1 channel) will also be produced.

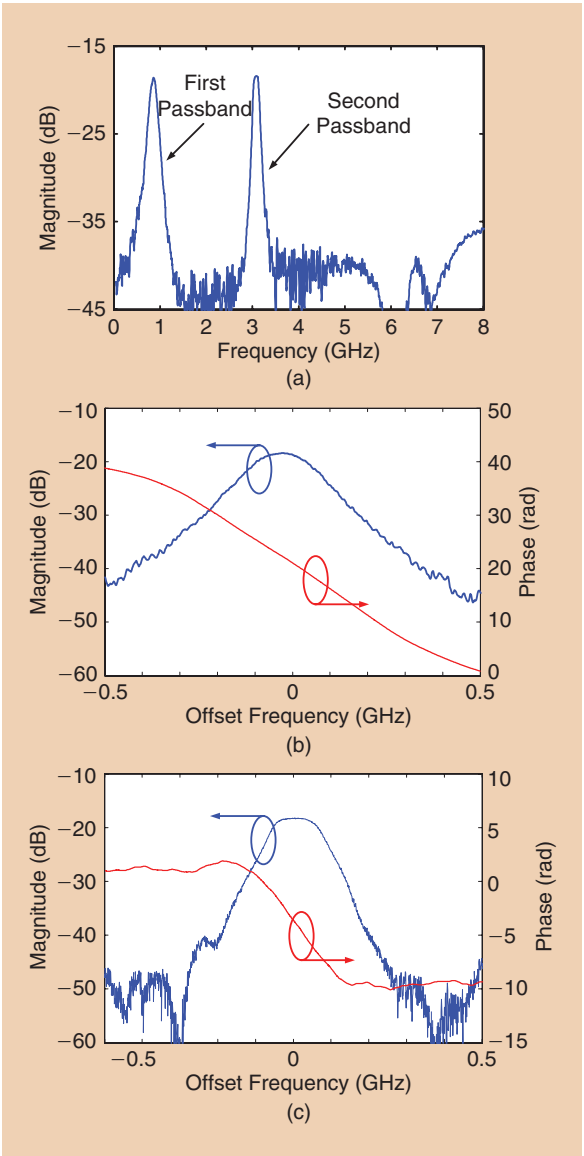

Figure 23. *(a) The frequency response of the dual-passband microwave photonic filter. (b) The frequency response and phase response of the first passband. (c) The frequency response and phase response of the second passband [35].*

Therefore, there will be two passbands with central frequencies of ω_1 and ω_2. The central frequencies of the passbands can be tuned by shifting the wavelengths of TLS 1 and TLS 2 independently.

Figure 23 shows the spectral response of the dual-passband filter. The bandwidth and shape factor of the first passband are 167.3 MHz and 3.8, respectively, and those of the second passband are 143.4 MHz and 3.3. The first and second passbands have frequency tunable ranges of 5.4 and 7.4 GHz, respectively. The central frequencies of both passbands can be continuously tuned. Again, the shape of the spectral response of the two passbands is unchanged during tuning. The variations of the magnitude over the tunable ranges are maintained within ±0.5 dB.

The SFDRs for the two passbands and the noise figures (NFs) of the filter are two important parameters that define the performance of the filter. The SFDRs and the NFs can be improved if the optical carriers are partially suppressed while keeping the power to the PD unchanged. This operation is equivalent to increasing the filter gains. This can be done using an SBS-assisted filter, as shown in Figure 22.

The SBS-assisted filter is implemented using a dispersion-shifted fiber (DSF). When the light waves pass through the DSF and the powers of the optical carriers are above the SBS threshold, Stokes waves are generated, which travel along the DSF in the opposite direction of the optical carriers. Note that, under small-signal modulation conditions, the powers of the sidebands are below the SBS threshold; thus, SBS occurs only at the optical carriers, and the sidebands are kept unchanged.

The Stokes waves go through PC 3, which is used to adjust their polarization state, and then they are launched into the DSF via OC 2. As the Stokes waves consecutively circulate in the ring, the optical carriers are suppressed. When the optical power at the input of the PD is constant, the suppression of the optical carriers will increase the gain of the system. The SFDRs for the two passbands are 82.9 and 83.2 $dB \cdot Hz^{2/3}$, when the SBS-assisted filter is not incorporated into the system. After connecting PC 3 with port 1 of OC 2, the optical carriers are partially suppressed, and when the optical power at the input of the PD is kept identical to the optical power without carrier suppression, the gain of the system is improved by about 10 dB. The measured SFDRs of the first and second passbands are then 89.8 and 90.6 $dB \cdot Hz^{2/3}$, respectively, an improvement of about 7 dB, and the NFs of the two passband filters are decreased by 10 dB.

Conclusion

An overview of microwave photonic filters implemented in both the incoherent and coherent operational regimes has been provided. For microwave photonic filters implemented in the incoherent regime, an incoherence light source—usually a broadband light source such as a light-emitting diode source, an amplified spontaneous emission source, or a laser array—is needed. The problem of using a broadband light source is the low optical power and high noise, which may cause the microwave photonic filters to have a very poor NF. The use of a laser array can avoid the problem, but the cost is high. In addition, the tuning of the filter is usually performed by tuning the wavelengths of the laser array, which is very complicated (the wavelength spacing must be tuned). In addition, the implementation of an incoherent microwave photonic filter with an arbitrary spectral response requires the filter to have complex coefficients, which are hard to realize. The use of the nonuniform tap spacing concept can simplify the implementation, but the complex coefficients are realized via changing the tap spacing that is frequency-dependent and accurate only for a specific frequency, and thus the frequency response is precise for narrowband operation.

An effective solution to increase the dynamic range is to cancel the third-order intermodulation terms.

On the other hand, the implementation of microwave photonic filters in the coherent regime can have a much simpler configuration. The filter spectral response is, in fact, the spectral response of an optical filter that is translated into the microwave domain. Thus, the key to implementing a coherent microwave photonic filter is to design an optical filter with a well-defined spectral response. Tuning coherent microwave photonic filter can be simply accomplished by tuning the wavelength of the coherent light source.

Although both incoherent and coherent microwave photonic filters offer the advantages of high operating frequency and large frequency tuning, the filters usually have high insertion loss, poor NF, and a small dynamic range. The use of a high-power-handling PD may reduce the insertion loss and increase the noise performance, but the dynamic range can only be improved by using techniques such as prelinearization or postlinearization, which should be done in the electronic domain, making the filters complicated and costly. An effective solution to increase the dynamic range is to cancel the third-order intermodulation terms—a technique has been used for microwave photonic links [36].

Almost all microwave photonic filters reported in the literature were implemented using discrete optoelectronic and microwave components. Thus, the size is large, the overall performance is limited, and the cost is high. Using integrated photonic circuits should be a solution to improve performance and to reduce size and cost. For example, an integrated tunable optical delay line was implemented using a CMOS-compatible photonic circuit, and the delay line was then used to demonstrate a microwave photonic filter [37].

However, although the size is reduced, current silicon photonic technology does not allow full integration of the entire filter system, especially the light source, which cannot be produced using silicon since silicon is an indirect bandgap material and thus will produce no light emission. To produce effective light emission, direct bandgap materials must be used. One possible solution is to employ hybrid integration, to produce light emission and light amplification using a direct bandgap material and using silicon for other functions (modulation, time delay, and photodetection). With this hybrid approach [38], fully integrated microwave photonic filters would perform better and be ready for practical applications.

References

[1] K. Wilner and A. P. van den Heuvel, "Fiber-optic delay lines for microwave signal processing," *Proc. IEEE*, vol. 64, no. 5, pp. 805–807, May 1976.

[2] E. C. Heyde and R. A. Minasian, "A solution to the synthesis problem of recirculating optical delay line filter," *IEEE Photon. Technol. Lett.*, vol. 6, no. 7, pp. 833–835, July 1994.

[3] J. Capmany, J. Cascon, J. L. Martin, S. Sales, D. Pastor, and J. Marti, "Synthesis of fiber-optic delay line filters," *J. Lightwave Technol.*, vol. 13, no. 10, pp. 2003–2012, Oct. 1995.

[4] J. P. Yao, "Microwave photonics," *J. Lightwave Technol.*, vol. 27, no. 3, pp. 314–335, Feb. 2009.

[5] J. Capmany, B. Ortega, and D. Pastor, "A tutorial on microwave photonic filters," *J. Lightwave Technol.*, vol. 24, no. 1, pp. 201–229, Jan. 2006.

[6] R. A. Minasian, "Photonic signal processing of microwave signals," *IEEE Trans. Microwave Theory Tech.*, vol. 54, no. 2, pp. 832–846, Feb. 2006.

[7] J. Sancho, J. Bourderionnet, J. Lloret, S. Combrié, I. Gasulla, S. Xavier, S. Sales, P. Colman, G. Lehoucq, D. Dolfi, J. Capmany, and A. de Rossi, " Integrable microwave filter based on a photonic crystal delay line," *Natl. Commun.*, vol. 3, article 1075, pp. 1–9, Sept. 2012.

[8] V. R. Supradeepa, C. M. Long, R. Wu, F. Ferdous, E. Hamidi, D. E. Leaird, and A. M. Weiner, "Comb-based radiofrequency photonic filters with rapid tunability and high selectivity," *Natl. Photon.*, vol. 6, no. 5, pp. 186–194, May 2012.

[9] S. Sales, J. Capmany, J. Marti, and D. Pastor, "Experimental demonstration of fiber-optic delay line filters with negative coefficients," *Electron. Lett.*, vol. 31, no. 13, pp. 1095–1096, June 1995.

[10] F. Coppinger, S. Yegnanarayanan, P. D. Trinh, and B. Jalali, "All-optical RF filter using amplitude inversion in a semiconductor optical amplifier," *IEEE Trans. Microwave Theory Tech.*, vol. 45, no. 8, pp. 1473–1477, Aug. 1997.

[11] J. Capmany, D. Pastor, A. Martinez, B. Ortega, and S. Sales, "Microwave photonics filter with negative coefficients based on phase inversion in an electro-optic modulator," *Opt. Lett.*, vol. 28, no. 16, pp. 1415–1417, Aug. 2003.

[12] B. Vidal, J. L. Corral, and J. Marti, "All-optical WDM multi-tap microwave filter with flat bandpass," *Opt. Exp.*, vol. 14, no. 2, pp. 581–586, Jan. 2006.

[13] F. Zeng, J. Wang, and J. P. Yao, "All-optical microwave bandpass filter with negative coefficients based on a phase modulator and linearly chirped fiber Bragg gratings," *Opt. Lett.*, vol. 30, no. 17, pp. 2203–2205, Sept. 2005.

[14] J. Wang, F. Zeng, and J. P. Yao, "All-optical microwave bandpass filter with negative coefficients based on PM-IM conversion," *IEEE Photon. Technol. Lett.*, vol. 17, no. 10, pp. 2176–2178, Oct. 2005.

[15] J. P. Yao and Q. Wang, "Photonic microwave bandpass filter with negative coefficients using a polarization modulator," *IEEE Photon. Technol. Lett.*, vol. 19, no. 9, pp. 644–646, May 2007.

[16] Q. Wang and J. P. Yao, "Multi-tap photonic microwave filters with arbitrary positive and negative coefficients using a polarization modulator and an optical polarizer," *IEEE Photon. Technol. Lett.*, vol. 20, no. 2, pp. 78–80, Jan. 2008.

[17] A. Loayssa, J. Capmany, M. Sagues, and J. Mora, "Demonstration of incoherent microwave photonic filters with all-optical complex coefficients," *IEEE Photon. Technol. Lett.*, vol. 18, no. 16, pp. 1744–1746, Aug. 2006.

[18] A. Loayssa, R. Hernandez, D. Benito, and S. Galech, "Characterization of stimulated Brillouin scattering spectra by use of optical single-sideband modulation," *Opt. Lett.*, vol. 29, no. 6, pp. 638–640, Mar. 2004.

[19] Y. Yan and J. P. Yao, "A tunable photonic microwave filter with a complex coefficient using an optical RF phase shifter," *IEEE Photon. Technol. Lett.*, vol. 19, no. 19, pp. 1472–1474, Sept. 2007.

[20] Y. Dai and J. P. Yao, "Nonuniformly-spaced photonic microwave delay-line filter," *Opt. Expr.*, vol. 16, no. 7, pp. 4713–4718, Mar. 2008.

[21] F. Zeng and J. P. Yao, "All-optical bandpass microwave filter based on an electro-optic phase modulator," *Opt. Exp.*, vol. 12, no. 16, pp. 3814–3819, Aug. 2004.

[22] F. Zeng and J. P. Yao, "Investigation of phase modulator based all-optical bandpass microwave filter," *J. Lightwave Technol.*, vol. 23, no. 4, pp. 1721–1728, Apr. 2005.

[23] Y. Dai and J. P. Yao, "Nonuniformly spaced photonic microwave delay-line filters and applications," *IEEE Trans. Microwave Theory Tech.*, vol. 58, no. 11, pp. 3279–3289, Nov. 2010.

[24] Y. Dai and J. P. Yao, "Microwave pulse phase encoding using a photonic microwave delay-line filter," *Opt. Lett.*, vol. 32, no. 24, pp. 3486–3488, Dec. 2007.

[25] Y. Dai and J. P. Yao, "Chirped microwave pulse generation using a photonic microwave delay-line filter with a quadratic phase response," *IEEE Photon. Technol. Lett.*, vol. 21, no. 9, pp. 569–571, May 2009.

[26] Y. Dai and J. P. Yao, "Microwave correlator based on a nonuniformly spaced photonic microwave delay-line filter," *IEEE Photon. Technol. Lett.*, vol. 21, no. 14, pp. 969–971, July 2009.

[27] X. Yi and R. A. Minasian, "Microwave photonic filter with single bandpass response," *Electron. Lett.*, vol. 45, no. 7, pp. 362–363, Mar. 2009.

[28] J. Palací, G. E. Villanueva, J. V. Galán, J. Martí, and B. Vidal, "Single bandpass photonic microwave filter based on a notch ring resonator," *IEEE Photon. Technol. Lett.*, vol. 22, no. 17, pp. 1276–1278, Sept. 2010.

[29] D. Marpaung, R. Pant, B. Morrison, and B. J. Eggleton, "Frequency agile microwave photonic notch filter with anomalously-high stopband rejection," *Opt. Lett.*, vol. 38, vol. 21, pp. 4300–4303, Nov. 2013.

[30] X. Han and J. P. Yao, "Bandstop-to-bandpass microwave photonic filter using a phase-shifted fiber Bragg grating," submitted for publication.

[31] W. Li, M. Li, and J. P. Yao, "A narrow-passband and frequency-tunable microwave photonic filter based on phase-modulation to intensity-modulation conversion using a phase-shifted fiber Bragg grating," *IEEE Trans. Microwave Theory Tech.*, vol. 60, no. 5, pp. 1287–1296, May 2012.

[32] T. Erdogan, "Fiber grating spectra," *J. Lightwave Technol.*, vol. 15, no. 8, pp. 277–1294, Aug. 1997.

[33] L. Gao, X. Chen, and J. P. Yao, "Microwave photonic filter with a narrow and flat-top passband," *IEEE Microwave Wireless Compon. Lett.*, vol. 23, no. 7, pp. 362–364, July 2013.

[34] Y. Dai, X. Chen, D. Jiang, S. Xie, and C. Fan, "Equivalent phase shift in a fiber Bragg grating achieved by changing the sampling period," *IEEE Photon. Technol. Lett.*, vol. 16, no. 10, pp. 2284–2286, Oct. 2004.

[35] L. Gao, J. Zhang, X. Chen, and J. P. Yao, "Microwave photonic filter with two independently tunable passbands using a phase modulator and an equivalent phase-shifted fiber Bragg grating," *IEEE Trans. Microwave Theory Tech.*, vol. 62, no. 2, pp. 380–387, Feb. 2014.

[36] W. Li, F. Kong, and J. P. Yao, "Dynamic range improvement of a microwave photonic link based on bi-directional use of a polarization modulator in a Sagnac loop," *Opt. Exp.*, vol. 21, no. 13, pp. 15692–15697, July 2013.

[37] M. Burla, D. A. I. Marpaung, L. Zhuang, C. G. H. Roeloffzen, M. R. Khan, A. Leinse, M. Hoekman, and R. G. Heideman, "On-chip CMOS compatible reconfigurable optical delay line with separate carrier tuning for microwave photonic signal processing," *Opt. Exp.*, vol. 19, no. 22, pp. 21475–21484, Oct. 2011.

[38] M. J. R. Heck, J. F. Bauters, M. L. Davenport, J. K. Doylend, S. Jain, G. Kurczveil, S. Srinivasan, Y. Tang, and J. E. Bowers, "Hybrid silicon photonic integrated circuit technology," *IEEE J. Select. Topics Quantum Electron.*, vol. 19, no. 4, article 6100117, July–Aug. 2013.